

Cellulose nano- and micro-fibers as air lime carbonation accelerators: FTIR analysis of the carbonation kinetics

Paulina Guzmán García Lascurain^{a,*}, Carlos Rodríguez-Navarro^b, Mario Pagliaro^c,
Lucia Toniolo^a, Sara Goidanich^a

^a Department of Chemistry, Materials and Chemical Engineering "Giulio Natta", Politecnico di Milano, Piazza Leonardo da Vinci, 32, Milano 20133, Italy

^b Department of Mineralogy and Petrology, University of Granada, Fuentenueva s/n, Granada 18002, Spain

^c Istituto per lo Studio dei Materiali Nanostrutturati, CNR, via U. La Malfa 153, Palermo 90146, Italy

ARTICLE INFO

Keywords:

Air lime mortars
Cellulose additives
Carbonation acceleration
Slaking addition
FTIR

ABSTRACT

Air lime mortars are reemerging as an alternative sustainable material for construction and restoration of built heritage. However, their widespread use is still limited by the long hardening times, via carbonation, and limited early strength. A possible sustainable strategy to accelerate the carbonation process and early strength development of these mortars is using natural organic additives, such as submicrometric cellulose fibers. In this study, the effect of three cellulose additives on the carbonation kinetics of air lime mortars is presented. Furthermore, the effect of the cellulose time of addition on the carbonation process was evaluated. Additives were included both during the slaking process and to a hydrated lime paste. Results show that the cellulose fibers accelerate the carbonation of air lime mortars, particularly in the case of micro-cellulose and of micronized CitroCell cellulose sourced from citrus processing waste. When additives are included during slaking, their acceleration effect on carbonation is enhanced. These outcomes suggest that the addition of cellulose additives can enhance both the rate and depth of carbonation, potentially improving the performance and durability of the mortars. It should be considered and further investigated that addition during slaking might be advantageous not only for cellulose but also for other kind of additives.

1. Introduction

The interest in using air lime mortars in construction has increased in recent years due to their carbon sequestration capacity and potential to reduce their environmental impact [1,2]. Furthermore, air lime is one of the materials of choice by restorers for the conservation of built heritage, amongst other options such as earthen and natural hydraulic mortars. Air lime generally presents a good compatibility with historical masonry in terms of physical, chemical, and aesthetic properties [3,4].

Despite the increasing interest, the quality and performance of air lime binders, especially in terms of the setting and hardening times, remain debated compared to hydraulic lime binders. This is because of the prolonged setting times of air lime via carbonation, and lower mechanical strength compared with hydraulic lime mortars. These are determining factors of the lime quality and overall performance as a binder [5].

High calcium air lime is produced from pure limestones (CaCO_3 content > 94 % [6]). These are calcinated to obtain quicklime (CaO) and

then hydrated to form Ca(OH)_2 [7]. To form a mortar, quicklime or calcium hydroxide should be slaked/mixed (respectively) in excess of water to form a moldable paste known as *lime-putty* that can be integrated with aggregates and additives (if required). Once casted or set in place, the mortar will dry via evaporation gaining some initial strength due to capillary forces [8]. At this stage, the process of carbonation will initiate, progressing from the surface to the bulk of the material [9].

Carbonation is a diffusion/dissolution-controlled process depending on different factors [9]. It takes place thanks to diffusion of CO_2 and moisture through the open pore network of the mortar [8,10]. The carbonation front advances from the surface to the bulk of the material and consists of the following steps [9,11]: i) firstly, Ca(OH)_2 (s) will be dissolved into the pore water and the $\text{Ca}_{(\text{aq})}^{2+}$ and $\text{OH}_{(\text{aq})}^-$ ions will dissociate. This increases the pH of the pore solution (up to a maximum pH of 12.4). Then, ii) CO_2 (g) will be dissolved into this alkaline pore solution, and iii) interact with the $\text{OH}_{(\text{aq})}^-$ to form HCO_3^- (aq) and CO_3^{2-} (aq). Finally, iv) the carbonate ions will react with the Ca^{2+} (aq) ions present in the pore solution and precipitate as CaCO_3 . Overall, this is a slow

* Corresponding author.

E-mail address: paulina.guzman@polimi.it (P. Guzmán García Lascurain).

<https://doi.org/10.1016/j.conbuildmat.2025.142291>

Received 3 March 2025; Received in revised form 19 May 2025; Accepted 13 June 2025

Available online 17 June 2025

0950-0618/© 2025 The Author(s). Published by Elsevier Ltd. This is an open access article under the CC BY license (<http://creativecommons.org/licenses/by/4.0/>).

process, know to require years to be completed [12]. Rodríguez-Navarro et al. [9] distinguished three main factors impacting the notably slow kinetics of this process in mortars: temperature, relative humidity (RH) and CO₂ concentration. For an optimal carbonation rate, temperature should range between 17 – 20 °C [8,13]. Relative humidity should be between 40 – 80 % [8] to allow CO₂ diffusion and dissolution of the reacting species. Finally, the CO₂ concentration [CO₂] should not exceed 20 % [14,15] (500 times the atmospheric concentration).

Additives are a common solution to accelerate carbonation [16]. These are often incorporated during mortar mixing, and their mechanisms of action can vary [9] affecting the carbonation process in different manners. Water-retaining additives can modify the internal RH of the mortar, promoting carbonation, while others alter the porous structure to accelerate the process. Additionally, carbonation can be further enhanced by optimizing carbonation chemistry.

For instance, TiO₂, is a commonly used self-cleaning additive that also provides an external source of CO₂ and water in the mortar surface following photocatalytic degradation of deposited organic pollutants [17]. However, the carbonation acceleration results reported in the literature may vary. For example, Karatasios et al. [17] observed an increment of less than 2 % of CaCO₃ content as compared with an additive-free control whereas others [18,19] revealed a marked acceleration of the carbonation, especially when subjected to UV irradiation.

Natural organic additives can also be used to speed up the carbonation process. For example, exploiting the fermentation process of organic matter [20–22] to provide an external source of CO₂. The addition of fermented organic matter results in deeper carbonation front, with respect to the non-additivated mortar, and a corresponding improvement in mechanical properties [20–22]. Other organic additives like diethyl carbonate (DEC) [23] or carbonic anhydrase enzyme (CA) [11] can also be used as optimizers of carbonation chemistry. DEC provides an external source of carbonate ions that interact with the calcium ions in the pore solution [23]. This increases the carbonation rate and surface hardness. On the other hand, CA works by catalyzing the hydration of CO₂ to form HCO₃⁻, which is the rate limiting step in the overall carbonation reaction, thus accelerating carbonation kinetics [11]. As a result, the lime pastes with CA showed faster rates of carbonation, with an increase of 15 % in CaCO₃ as compared with a reference mortar.

Inspired by nature and history, Rodríguez-Navarro et al. [24–26] proposed a different approach to the use of organic additives. Instead of including these materials during the mortar mixing, they studied the effect of additivation during the formation of Ca(OH)₂ (i.e., during the slaking of quicklime). Their results confirm that in this manner, the organic molecules interact with the forming mineral and change the resulting size and crystal morphology, particularly making smaller plate-like portlandite crystals, much like those seen after lime putty aging [27]. These modifications have relevant implications for the carbonation acceleration, since the resulting morphologies are more reactive due to an increase in available surface area.

Cellulose fibers have been mainly tested previously with the scope of improving the mechanical resistance of mortars. Generally, an increase in the flexural resistance is obtained when the cellulose fibers are macro-sized [28–31]. Therefore, the use of nano- and micro-cellulose fibers, a common waste product of the textile industry [32], is an appealing sustainable alternative to macro-sized cellulose fibers. However, the use of these additives as mechanical reinforcement yielded inconclusive or contradictory results [33,34].

Nano- and micro-cellulose could be also used as additives to accelerate the carbonation process of air lime. In a recent work [35], it was demonstrated that nano- and micro-cellulose produce relevant morphological modifications to Ca(OH)₂ when included during the mineral formation (i.e., lime slaking). These changes are known to potentially favor the reactivity of the resulting material and could thus accelerate their carbonation. Furthermore, results on powder specimens [36] showed that these additives promoted a faster carbonation of Ca

(OH)₂. The present study aims to evaluate the effect of nano- and micro-cellulose fibers on the carbonation kinetics of pure air lime binders. Moreover, this work aims to unveil the effect that the addition timing (during Ca(OH)₂ formation or to a hydrated lime paste) of the additives has on the carbonation process.

2. Materials and methods

2.1. Raw Materials

The quicklime used in this work was characterized by a high CaO content (superior to 89 % – Table 1) and provided by Fassa Bortolo Srl, Italy. The reported values were obtained by X-ray diffraction (XRD, Table 1 and Figure S1) as specified in a previous work [35].

Three types of cellulose additives were employed: nano-, micro- and citro-cellulose (Figure S2 and Table S1). Nano-cellulose was synthesized via acid hydrolysis of commercial pure hydrophilic cotton and using the methodology reported by Vismara et al. [32]. The obtained product consists of crystalline nanocellulose fibers with an average size of 280 ± 56 nm (evaluated with Dynamic Light Scattering, DLS – Zetasizer Nano Instrument, Malvern Panalytical). Micro-cellulose, with trade name Microfibrillated cellulose – Celova ®, was kindly provided by Weidmann (Rapperswil, Switzerland). It is made up of amorphous fibers [35] 8 – 10 µm in size produced by intense mechanical grinding of pure cellulose pulp. Finally, citro-cellulose (CitroCell) was obtained via acoustic cavitation of industrial lemon processing waste carried out in water only [37]. The material is characterized by highly disordered rod-shaped cellulose fibers with a length of about 0.5–1.0 µm and a section of about 0.1–0.2 µm. Similarly to those obtained via hydrodynamic cavitation [38], the CitroCell fibers are substantially (ca. 40 %) esterified with citrate groups originating from citric acid present in lemon processing waste.

2.2. Production of the specimens

The progression of the carbonation reaction was measured in mortar specimens of 1 cm³ using air lime putty obtained from the slaking of quicklime. All the lime putties employed were slaked in the same day using a CaO: H₂O mass ratio of 1: 2.45. Deionized water at 25 °C was used for the slaking. The obtained putties were conserved in closed plastic bags for three months before using them. This ensured the complete hydration of the quicklime. All the mortars were prepared using quartz (SiO₂) sand as aggregate (granulometry 0.1 – 0.3 mm) (provided by Aquael – Acqua Decoris, Warsaw, Poland). The aggregate was mixed manually with the lime putty in a mass ratio of 1: 0.9 (lime putty: aggregate).

With the aim of understanding the effect that the addition timing of the cellulose additives had on the carbonation kinetics, two sets of mortar specimens were prepared:

- Set S: where the cellulose additives were included during the slaking process of quicklime. In this case, the additives were dispersed in the slaking water before adding the CaO.
- Set H: where the cellulose additives were added during the mortar manufacturing to the already hydrated lime putty. Here, the additives were mixed with the aggregates before adding the lime putty.

The control mortar specimens were made using a lime putty that had not been additivated with cellulose.

Once mixed, the series of 20 mortars per set were casted in silicone molds of 1 × 1 × 1 cm³ and left to carbonate in atmospheric conditions (~ 400 ppm [CO₂]). The mortars had only one exposed face, which forced the carbonation front to progress in a controlled direction.

Three concentrations of cellulose additives were tested for each additive and set: 100, 1000 and 5000 ppm. Table 2 presents a description of the nomenclature used.

Table 1
Quantitative XRD characterization of the quicklime used to make the mortar specimens [35].

CaO	Calcite	Portlandite	Anhydrite	Periclase	Quartz
90.2 ± 1.1	1.6 ± 0.1	5.8 ± 1.1	0.7 ± 0.1	1.7 ± 0.1	0.03 ± 0.01

Table 2
Nomenclature code to differentiate the different specimens used, classified by set and additives employed.

Name	Set	Additive	Concentration (ppm)		
Control	Control	No additive	–		
S Nano 100	Slaked	Nano-cellulose	100		
S Nano 1000			1000		
S Nano 5000			5000		
S Micro 100			Micro-cellulose	100	
S Micro 1000				1000	
S Micro 5000	5000				
S Citro 100	Citro-cellulose	Citro-cellulose	100		
S Citro 1000			1000		
S Citro 5000			5000		
H Nano 100	Hydrated	Nano-cellulose	100		
H Nano 1000			1000		
H Nano 5000			5000		
H Micro 100			Micro-cellulose	100	
H Micro 1000				1000	
H Micro 5000				5000	
H Citro 100			Citro-cellulose	Citro-cellulose	100
H Citro 1000					1000
H Citro 5000					5000

2.3. Quicklime characterization

The mineral characterization of the quicklime was done using a D8 Advance diffractometer (Bruker), at 45 kV and 40 mA on a range of 5–70 ° in 2θ, using Cu Kα radiation (λ = 1.5405 Å). The phase quantification was performed using the Rietveld refinement method [39] on DIFRAC.TOPAS software (Bruker).

2.4. Carbonation progression

The analysis of the carbonation progression was measured over a total period of 83 days. All the measurements were performed with Fourier Transformed Infrared Spectroscopy in attenuated total reflectance mode (FTIR – ATR) using a NicoletTM iS20 spectrometer (ThermoFisher Scientific, Waltham, MA, USA), equipped with a DTGS detector and a diamond iXTM Smart accessory for ATR (diameter of the crystal 2 mm), in the spectral range 4000–400 cm⁻¹, collecting 64 scans for each measurement with a 4 cm⁻¹ spectral resolution.

For each measuring day, one of the 10 replicas of the specimens was demolded and used in its totality. Before the analysis, the whole specimen was grinded in an agata mortar to obtain a fine powder that could be tested. The specimens were tested on the following days after the molding: 1, 2, 3, 7, 14, 21, 30, 50, 65, and 83.

Each measurement was conducted in triplicate, changing the powder that was being analyzed within the same specimen, and the average spectrum was considered. The progression of the carbonation reaction (that could only progress across the single exposed face of the cubic specimens) was evaluated considering the ratio between peak height of the carbonate peak (ν₃, asymmetric C-O stretching mode) at 1420 cm⁻¹ and the hydroxide peak (O-H stretching mode) at 3640 cm⁻¹ of the average spectra. The presence of CO₃ in these specimens can solely be originated from the conversion of Ca(OH)₂ to CaCO₃, thus making this ratio a reliable carbonation indicator. All the peak heights were calculated with OMNIC software (ThermoFisher Scientific) using an automatic linear baseline. The calculated ratio was nominated as “degree of carbonation” (DC) and is defined as:

$$DC_{t_x} = \left(\frac{I_{CO_3}}{I_{OH}} \right)_{t_x} \quad (1)$$

Where I_{CO_3} and I_{OH} are the corresponding peak intensities at any given time of measurement (t_x). It is important to note that the degree of carbonation (DC) is a relative measurement based on the specific set of specimens used in this study. Future research should consider establishing an equivalent DC value for any new set of specimens.

The relative fractional carbonation (FC) was calculated by normalizing DC_{t_x} with respect to the DC_{t_0} value of each set. In this case t_0 refers to the first day of measurement (day 1). The fractional carbonation is defined as:

$$FC = 1 - \frac{DC_{t_0}}{DC_{t_x}} \quad (2)$$

3. Results and discussion

The progression of carbonation of all tested specimens showed the expected progression over time (Fig. 1 and Fig. 2), with a fast conversion rate of Ca(OH)₂ to CaCO₃ during the early stages (≤ 21 days, before the plateau is reached for any set), that slows down over time, ultimately reaching a plateau. The carbonation kinetics should follow the second Fick's law of diffusion [8,9,40]:

$$DC = k_{Fick} \sqrt{t - 1} \quad (3)$$

When the degree of carbonation is considered, the process kinetics follows the second Fick's law of diffusion, as show in Fig. 1, where the carbonation extent shows a good fitting following Eq. (3). From this fitting the carbonation rate constant k_{Fick} for the different runs was calculated. The values are reported in Fig. 3. In all cases, k_{Fick} ranged from 2.0 ± 0.2–8.9 ± 0.5 day^{-0.5}, showing significant differences between the control ($k_{Fick} = 2.7 ± 0.2$ day^{-0.5}) and the mortars additivated with the three types of cellulose. Differences were also observed between the mortars with additives depending on the timing of additive dosing (before slaking and once the lime was hydrated), as is clearly observed in Fig. 3.

Moreover, when the fractional carbonation is considered (Fig. 2), the fast increment of carbonation at short times is more evident. To analyze these results, a simplified version of the Boundary Nucleation and Growth Model (BNGM kinetic model) [41–43] can be used. Originally, this kinetic model follows a sigmoidal behavior, and is based on the assumption that the conversion process occurs from the grain boundary to the center of the Ca(OH)₂ particles [41,42]. However, for the specific case of Ca(OH)₂ carbonation, it was shown [43] that a limiting case of the BNGM model, where the carbonation fraction changes exponentially with time, is more accurate to describe the process. The process kinetics (Fig. 2) was then also evaluated using the following relationship:

$$FC = 1 - \exp(k_{Exp}(1-t)) \quad (4)$$

For $t \geq 1$ days

Where k_{Exp} is an equivalent carbonation rate constant to k_{Fick} , and depicts an increment in the rate of the carbonation, especially at the initial period (i.e. before the plateau). The values of k_{Exp} reported in Fig. 3 show that k_{Exp} ranged from 0.1 ± 0.01–0.4 ± 0.02 day⁻¹. Here, the general behavior of the different mortar samples previously described for the case of k_{Fick} is maintained.

As shown in Fig. 4, the control specimen after 83 days was mainly

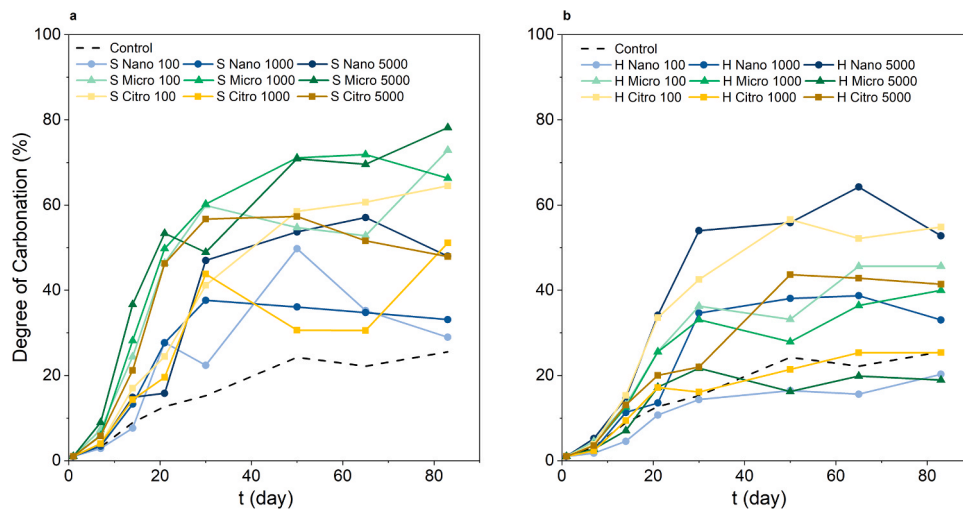


Fig. 1. Degree of carbonation (expressed as %) over 83 days of mortar specimens containing different quantities of nano-, micro- and citro-cellulose. The mortars were prepared dosing the additives during the slaking process, indicated by the prefix “S” (a) and to the mortar mixture with hydrated lime, indicated by the prefix “H” (b). The standard deviation of the results is not depicted in the graph for legibility; the standard deviation was on average 15 % of the measured value.

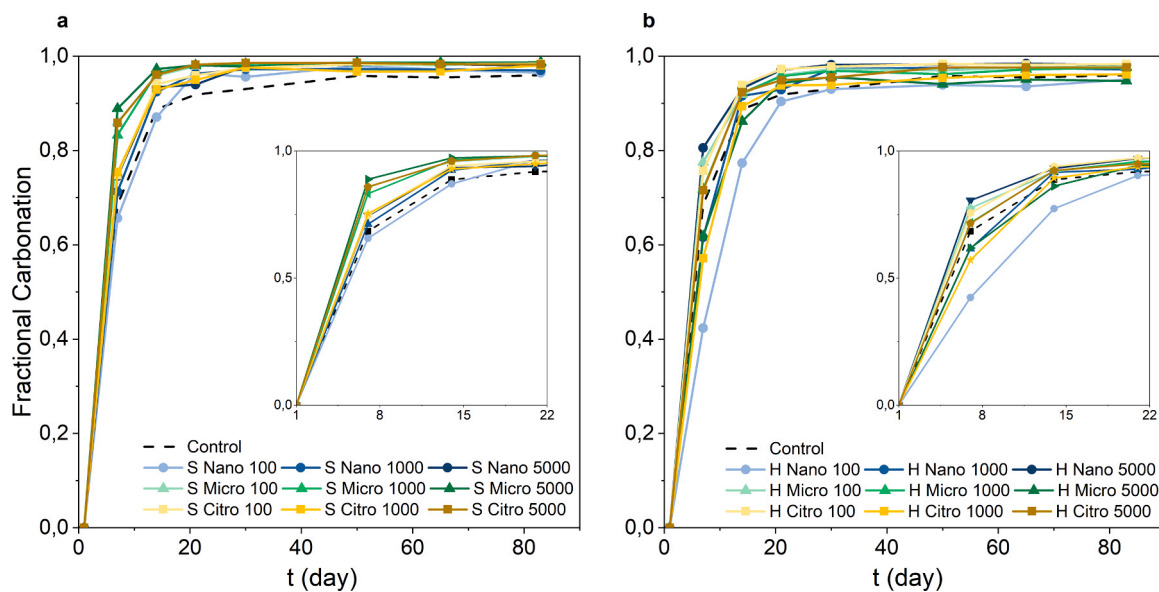


Fig. 2. Relative fractional carbonation for over 83 days of mortar specimens containing different quantities of nano-, micro- and citro-cellulose. The mortars were made including the additives during the slaking process, indicated by the prefix “S” (a) and to the mortar mixture with hydrated lime, indicated by the prefix “H” (b). The insets depict the first 21st days of carbonation.

constituted by calcite [44], however, a small peak of the hydroxyl group (3640 cm^{-1}) indicates the presence of a fraction of $\text{Ca}(\text{OH})_2$ in a few cases. This indicates that complete carbonation was not fully achieved.

Interestingly, the presence of cellulose additives resulted in an overall higher carbonation rate (Fig. 3) as compared with the control, except for a few single cases observed when cellulose was added to the hydrated paste. In the following paragraphs these results are discussed in detail.

3.1. Cellulose addition during the slaking process

As depicted in Fig. 1, the highest conversion rates are observed when cellulose was added during the slaking process (i.e. during the formation of $\text{Ca}(\text{OH})_2$) (Fig. 1a and Fig. 2a). Particularly, the increment is evident since the first day of carbonation. In all cases, there is a marked increase of the carbonation rate constants with respect to the control. The variation in the degree of carbonation observed at different days on some

sets is attributed to compositional changes in single replica specimen from a given set (the specimens were used in their totality for each measurement, see § Materials and Methods). After around 30 days of carbonation, the conversion rate of the additivated mortars becomes similar to the control. However, the $\text{CaCO}_3/\text{Ca}(\text{OH})_2$ ratio is significantly higher than the control and this difference is maintained throughout the whole experiment (Fig. 1a and Fig. 3a). To analyze the effect of the additives during the initial phase of carbonation, the carbonation rate constants k_{Fick} and k_{Exp} of the carbonation curves were then calculated as indicated above. The results (Fig. 3a) revealed that the carbonation rate is higher when using micro-cellulose, as compared with nano- and citro-cellulose. In fact, the average value of the carbonation rate constant k_{Fick} obtained for all the concentrations of micro-cellulose is 3 times higher than the control, and k_{Exp} is 1.7 times higher. Citro-cellulose also produces an acceleration, with k_{Fick} and k_{Exp} 66 % higher than the control, but only when used in the highest dosage (5000 ppm), and to a lower extent than micro-cellulose. In all other

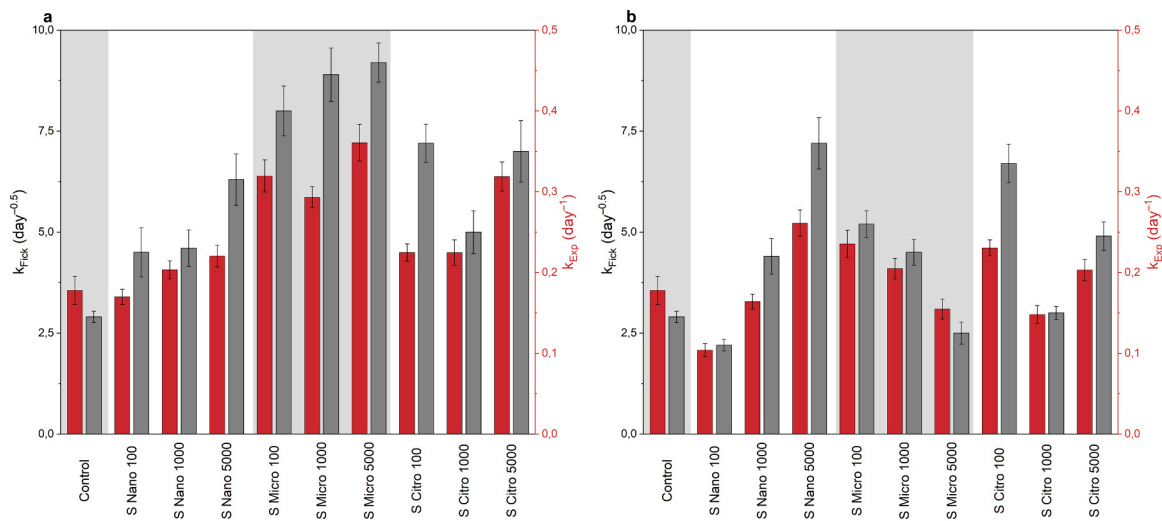


Fig. 3. Carbonation rate constants k_{Frick} (gray) and k_{Exp} (red) of the two fitting models applied to the degree of carbonation and relative fractional carbonation curves respectively for the control mortars, the (a) mortars with cellulose added during the slaking and (b) mortars with cellulose added to a hydrated paste. Error bars show standard deviation.

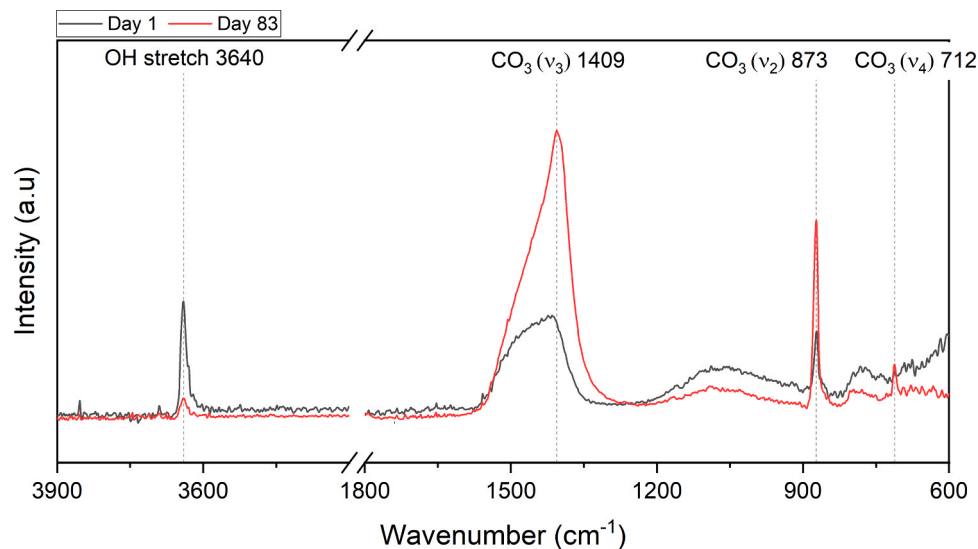


Fig. 4. FTIR spectra of the control mortars tested on the first and last day of the carbonation process. The wavenumbers correspond to the main vibrations of $\text{Ca}(\text{OH})_2$ and CaCO_3 in the reference specimens. Wavenumbers from 1800 to 3300 cm^{-1} are ignored since they do not provide any relevant information.

cases, the addition of cellulose during the lime slaking process incremented the rate of carbonation with respect to the control by at least 21 % (Fig. 3a). It is interesting to notice that citro-cellulose reaches high DC values after day 50 of carbonation when dosed at the lowest concentration of 100 ppm (Fig. 1a). This means that the set prepared with this concentration reaches a higher degree of CaCO_3 conversion, despite the fact that during the first 21 days of carbonation the acceleration rate was not the fastest compared with other sets. Results suggest that the citro-cellulose might provide optimal results both at high (5000 ppm) and low (100 ppm) concentrations, comparable to those obtained with micro-cellulose. This is an aspect that requires further investigation. It is important to underline that micro-cellulose showed the highest final degree of carbonation value, regardless of the concentration, while nano-cellulose only at the highest concentration (5000 ppm). In the following paragraphs an interpretation for these effects will be provided.

This is in line with previous results [36] of powder specimens from a homogeneous synthesis analyzed with FTIR and XRD. In that case [36], calcite was detected after 20 days only when $\text{Ca}(\text{OH})_2$ formed in the presence of nano- and micro-cellulose. Conversely, it was shown that the

control specimen at 20 days still presented vaterite and amorphous calcium carbonate (ACC), evidencing the incomplete carbonation [36].

A key factor to understand previous [36] and present results is the fact that in both cases cellulose was added during the formation of $\text{Ca}(\text{OH})_2$. Therefore, in this way it influences the mineral formation as it was clearly evidenced in another recent investigation [35]. There it was revealed that when cellulose is added during slaking, relevant morphological modifications are induced to the resulting $\text{Ca}(\text{OH})_2$. Thus, to understand the observed acceleration effect of the cellulose additives used in this work, it is important to take into consideration the obtained mineral morphology and particle size when the cellulose is added in the slaking process. A correlation of the obtained mineral morphologies/size and the carbonation rate is presented in Table 3.

As mentioned in the introduction, different pathways to increase the carbonation of $\text{Ca}(\text{OH})_2$ have been reported [9,16]. One of them is to modify the morphology of the mineral through the inclusion of additives [25,35]. In the case of cellulose [35], it was demonstrated that when highly crystalline nanofibers are present during the mineral formation, a larger portion of plate-like particles is produced; instead, amorphous

Table 3

Correlation between mineral morphology [35] and carbonation rate constants for each specimen type. For specimens containing cellulose additives, the reported value represents the average carbonation rate across all tested concentrations.

Additive	Mineral morphology [35]	$k_{\text{Fick}} [\text{day}^{-1/2}]$	$k_{\text{Exp}} [\text{day}^{-1}]$
No additive (control)	Crystalline, hexagonal micrometer prisms	2.7 ± 0.2	0.18 ± 0.02
Micro-cellulose	Amorphous nano- to micrometer-sized particles	8.4 ± 0.6	0.32 ± 0.03
Citro-cellulose	N.A.*	6.1 ± 1.2	0.26 ± 0.05
Nano-cellulose	Crystalline, hexagonal plate-like nanoparticles	4.9 ± 1	0.2 ± 0.03

* In [35] the effect of citro-cellulose was not tested and thus it is not included in this table.

cellulose microfibrils stabilize a *dense liquid mineral precursor*. This precursor is a highly hydrated mineral phase formed after liquid-liquid phase separation in solution [26,45,46]. Upon dehydration, the liquid mineral can produce amorphous or crystalline calcium hydroxide. The formation of either of these solid phases depends on the dehydration rate, a fast process will yield amorphous calcium hydroxide (ACH) whereas a slow rate will produce crystalline $\text{Ca}(\text{OH})_2$. In summary, crystalline nanocellulose will yield crystalline plate like portlandite, whereas amorphous micro-cellulose and a fast dehydration rate of the dense liquid precursor (like that observed in the products of a typical slaking reaction) will produce ACH.

The different cellulose additives used can be then classified in terms of their crystallinity, which will impact the resulting mineral morphology of $\text{Ca}(\text{OH})_2$. The acid hydrolysis process that was used to obtain nano-cellulose is known to produce a larger portion of crystalline domains in the fibers [35]. In contrast, mechanical and cavitation methods used to produce micro- and citro-cellulose, respectively, produce mainly amorphous fibers [47,48]. Remarkably, CytoCell is not only poorly crystalline but it is also comprised of β 1–4 linked D-glucopyranose units in which about 40 % of glucose moieties are esterified with negatively charged citrate groups [49].

Therefore, the accelerated carbonation process can be associated with an increment in the $\text{Ca}(\text{OH})_2$ reactivity due to the morphological modifications induced by the cellulose fibers. But such morphological modifications can only be induced if the additives act on the nucleation and growth of $\text{Ca}(\text{OH})_2$. No effect on the already formed $\text{Ca}(\text{OH})_2$ crystals in hydrated lime is thus expected upon contact with the additives. The larger effect observed when using micro- and citro-cellulose fibers dosed during the lime slaking process can be also attributed to the presence of ACH. Generally, amorphous phases are more reactive than their crystalline counterpart [50–52] due to their thermodynamically metastable nature [53]. Consequently, a lime paste containing ACH will carbonate faster than one containing purely crystalline calcium hydroxide. Also, potentially, the intricate morphologies normally formed by ACH and its nanosize nature may contribute to an increment in the available surface area, and thus the reactivity.

On the other hand, the reactivity increment obtained for specimens made with nano-cellulose is lower than that observed with micro-cellulose, but still higher than the control (up to two times). In this case, the formation of crystalline plate-like nanoparticles was previously observed [35,36], differently than the crystalline rod-like $\text{Ca}(\text{OH})_2$ of the control [12,27,54]. When additives, such as nano-cellulose, are adsorbed in the {00.1} basal planes of the crystal, the mineral growth along the [001] direction will be hindered, provoking the preferential formation of platelets. This can be considered equivalent to opening new

surfaces in a prismatic crystal, which ultimately increments the available surface area to react and carbonate. Interestingly, this latter shape transformation can be seen when using other organic additives [25,55], and upon lime-putty aging [12,27,54]. This size and shape modifications of the $\text{Ca}(\text{OH})_2$ particles increment the available surface area with respect to the control, and as a consequence also the reactivity.

3.2. Cellulose added to the hydrated paste

The carbonation progression of the mortars made with cellulose added to an already hydrated lime paste is presented in Fig. 1b and Fig. 2b. In this case, a different effect on the carbonation kinetics of the mortar specimens is observed. During the first 14 days, the progress of carbonation of all tested specimens is comparable to that of the control. Only after this time, a positive effect of additives can be observed, which is maintained for the whole duration of the experiment. The only specimens where the addition of cellulose did not accelerate carbonation were nano-cellulose at 100 ppm, micro-cellulose at 5000 ppm and citro-cellulose at 1000 ppm. Since for this sets of specimens the cellulose additives were included once the lime was slaked, it is possible that specimen manufacturing could have played a relevant part in the results. It is important to remark that mortars were mixed manually, and even though the same hand was used during mixing, slight differences in the dispersion of the fibers for the H sets could have influenced the change in the observed dynamics.

To compare the results obtained from the different addition times of the cellulose, carbonation rate constants were used. At the initial stage (≤ 21 days), the cellulose added to the hydrated paste accelerated the reaction (Fig. 3b) by 14–82 % with respect to the control. However, as mentioned above, the effect of cellulose when added to a hydrated paste, does not start at the beginning of the carbonation. Therefore, evaluating the carbonation rate only at the initial phase of the process would not fully describe the real effect of the additives. In this case, the specimens with cellulose started to carbonate with an accelerated rate at around day 14 (Fig. 1b). Also in this case, after around 30 days, the carbonation rate of the mortars with cellulose becomes similar to the control but with higher values of degree of carbonation (Fig. 1b). Although the carbonation ratios were lower than those observed when cellulose was added during slaking. These results highlight the distinctive and positive outcome of adding cellulose at different times of the mortar production (i.e., during slaking).

When the additives are included to an already hydrated paste, it is possible to ensure that the fibers will not induce any morphological modifications to the minerals. Nonetheless, they do accelerate the carbonation reaction.

Two of the most important factors for carbonation to take place are the presence of CO_2 and humidity. In natural conditions, however, the internal RH of mortars tends to decrease over time, which is one of the limiting factors related to carbonation [7], resulting in materials with carbonated surfaces and uncarbonated cores. Thus, it would be ideal to not only accelerate the carbonation process but also doing it so in the volume fraction where it is most needed, i.e. the core of the mortar.

Interestingly, results show that the presence of the additives allows to maintain a high carbonation rate for longer a time. A possible explanation for this finding lies in the hydrophilic nature of cellulose that facilitates absorption of free water, acting as a *water reservoir*. This can aid to maintain higher levels of internal RH for a longer period of time. Incrementing the RH in the bulk of the mortar, where is most needed, is particularly necessary. Since the cellulose fibers are distributed throughout the whole volume of the mortar, it is reasonable to think that the proposed *water reservoir* capacity could aid to promote carbonation in the bulk. Another possible effect of the cellulose fibers may be that they act as pore-network modifiers. In this way, CO_2 could be transported easily from the surface to the inside of the specimen. Further analyses, such as electron microscopy, x-ray tomography or mercury intrusion porosimetry (MIP), are required to fully understand

the underlying mechanisms taking place in this case.

3.3. Implications of cellulose addition in air lime-mortars

The carbonation process is crucial since mortar strength, porosity and moisture transport properties will be affected by the degree of carbonation, ultimately determining the overall performance and durability of the composite [11]. Furthermore, carbonation allows to recapture CO_2 formed during lime calcination, thus reducing the overall CO_2 burden of this material [1], keeping in mind that other processes such as extraction, transportation, and disposal, also produce emissions.

In Fig. 5, a visualization of the effect that the carbonation rate constants, k_{Fick} and k_{Exp} , have on the overall process kinetics is depicted. In the mortars studied in the present work, the k_{Fick} and k_{Exp} values increased by a factor of two or even three with respect to the control. In both cases, a higher value of the constants depicts an acceleration of the process. When the carbonation rate constant is doubled, a substantial acceleration of the process is observed. It is important to point out that the main difference between the two models used is inherent description of the carbonation phenomena. The Fick model is based on the description of a diffusion-controlled process (i.e. CO_2 diffusion within the mortar's pore system). On the other hand, the Boundary Nucleation and Growth Model (BNGM) considers the nucleation and growth of the product phase (CaCO_3) on the reactant phase ($\text{Ca}(\text{OH})_2$). Naturally, the effect of a higher carbonation rate is more evident at the early stages of carbonation.

A mortar that carbonates faster would allow a faster CO_2 recapturing, making air lime-mortars a more efficient *carbon sink*. Furthermore, submicrometric cellulose additives such as citro-cellulose, can be sourced from waste materials. Re-integrating waste materials into a production chain is one strategy to reduce the environmental impact of additives.

Moreover, a faster carbonation process under atmospheric conditions could provide a faster development of the mechanical resistance of the mortars [15] both in the surface and bulk of the material. This could in turn make air lime mortar more resilient in a shorter time, favouring their use for built heritage restoration as well as modern construction. In addition to the carbonation acceleration, the cellulose fibers, when integrated during the slaking, might contribute to the mechanical reinforcement of mortars. Indeed, one of the characteristics of minerals formed in the presence of organic additives is that of an incremented mechanical resistance [56,57]. For the specific case of nano-cellulose, Lu et al. [58] demonstrated that a nanostructured organic-inorganic hybrid

mineral made in the presence of nano-cellulose had higher surface hardness and compressive strength than a conventional sticky rice lime mortar.

It is important to point out the dual effect that carbonation has on the mortar durability. Firstly, the carbonation of air lime mortars is critical for their resistance to environmental factors and overall durability [5]. An uncarbonated mortar will not resist weathering agents as much as a carbonated one. In this way, attaining a higher degree of carbonation in a shorter time can delay the detrimental effect of weathering and increase the overall durability. Therefore, a future perspective of this work should be to test the effect that the addition of cellulose, and the resulting faster carbonation, can have on durability-related material properties. For example, mechanical tests, including surface mechanical resistance, should be performed, together with porosimetry measurements and weathering degradation simulations (e.g., rain resistance, salt-crystallization resistance, and freeze/thaw cycles).

On the other hand, a fundamental result of this study is the clear difference between adding cellulose during the slaking process or to an already hydrated paste. The difference lies in cellulose capacity to modify the size, morphology, and phase (amorphous vs. crystalline) $\text{Ca}(\text{OH})_2$ exclusively when it is added during the mineral formation. Archaeometric evidence [24] has shown that the *slaking additivation* was a common practice of Maya masons; and the still standing buildings in the harsh tropical environment of the Maya area are testament of the air lime mortar long durability. Accordingly, more research is needed to evaluate the effect of additives included during the slaking of air lime.

Finally, in this study the best results were obtained for *slaking additivation*. In a previous work [35] from our group it was demonstrated that the morphological (and phase) modifications produced by cellulose additivation during slaking yielded a more reactive air lime. But this does not exclude the possibility of adding the cellulose also to a hydrated paste, where a positive outcome was obtained in most cases. In this way, both positive effects could be combined. Furthermore, this *dual additivation* does not complicate the mortar production process, since the same additive can be dosed to the slaking water and to the hydrated paste.

4. Conclusions

In the present work an analysis of the effect that different cellulose additives have on the carbonation kinetics of air lime mortars was performed. Furthermore, the effect that addition timing has on the carbonation was also investigated.

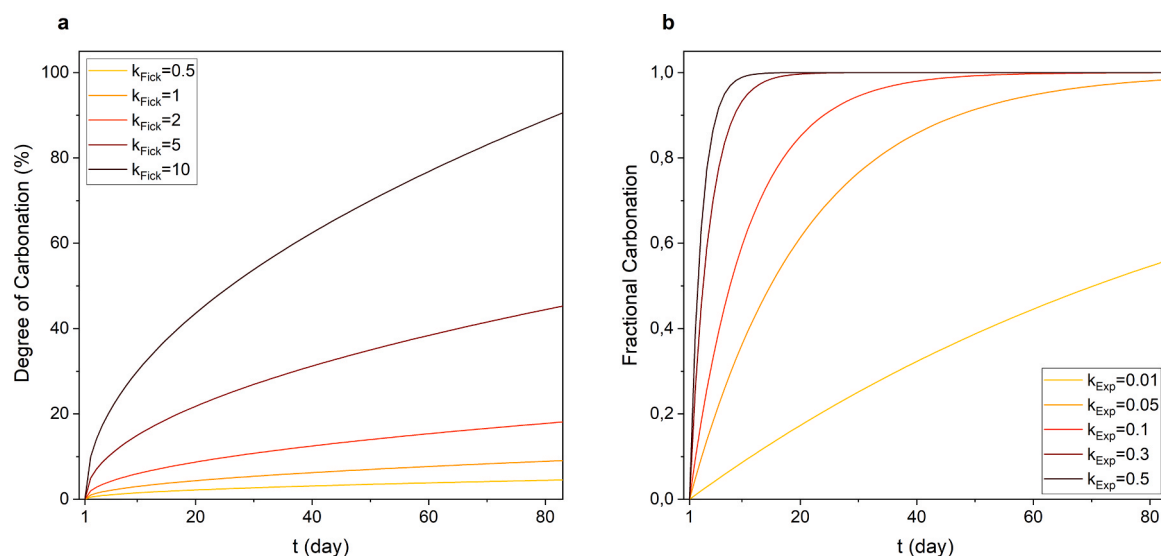


Fig. 5. Modeled effect that the k_{Fick} and k_{Exp} constants have on (a) the degree of carbonation and (b) the fractional carbonation respectively.

The results show that the addition of cellulose fibers (nano-cellulose, micro-cellulose and micronized cellulose from citrus processing waste) to air lime-mortars enhances the carbonation rate allowing to attain a higher degree of CO₂ capture in shorter times. Mortars made with micro-cellulose at 1000 ppm dosage and lemon submicronized cellulose (CitroCell) at 5000 ppm carbonated three times faster than the control. The increased carbonation rates of the mortars with micro-cellulose are linked to the presence of this highly reactive amorphous material.

The experimental results showed also that if the additives are included during the hydration of quicklime (i.e., slaking reaction), the effect is more relevant than when the additives are included to a hydrated paste. This distinctive effect is attributed to the previously demonstrated capacity that cellulose fibers have to modify the morphology, size and phase of Ca(OH)₂ during its formation [35].

On the other hand, when cellulose is added to an already hydrated paste, no morphological modifications of Ca(OH)₂ particles are expected to occur. In this case, the observed increment of the carbonation rate is hypothesized to be associated with a cellulose-mediated increment in the bulk RH, and a possible modification in the pore network of the mortar, although further investigation is required to confirm these hypotheses. Should these be verified, the mentioned effects are also expected to play a positive role in the case of the mortars prepared with cellulose added during the slaking process.

The results obtained in this study highlight the positive outcome obtained from *slaking additivation*, which is not exclusive of cellulose. Therefore, encouraging future research to extend the knowledge here presented, and include other additives in this way for the production of air lime mortars.

CRediT authorship contribution statement

Paulina Guzmán García Lascurain: Writing – original draft, Visualization, Validation, Methodology, Investigation, Funding acquisition, Formal analysis, Data curation, Conceptualization. **Mario Pagliaro:** Writing – review & editing, Resources. **Carlos Rodríguez-Navarro:** Writing – review & editing, Validation, Supervision, Investigation. **Sara Goidanich:** Writing – review & editing, Validation, Supervision, Resources, Project administration, Methodology, Funding acquisition, Conceptualization. **Lucia Toniolo:** Writing – review & editing, Validation, Supervision, Resources, Methodology, Funding acquisition, Conceptualization.

Declaration of Competing Interest

The authors declare the following financial interests/personal relationships which may be considered as potential competing interests: Paulina Guzmán García Lascurain reports financial support was provided by Italian PON Ricerca e Innovazione 2014–2020. Carlos Rodríguez-Navarro reports financial support was provided by HORIZON EUROPE Marie Skłodowska-Curie Actions. Carlos Rodríguez-Navarro reports financial support was provided by Spanish Government. Carlos Rodríguez-Navarro reports financial support was provided by Junta de Andalucía research group. Carlos Rodríguez-Navarro reports financial support was provided by University of Granada, Unidad Científica de Excelencia. If there are other authors, they declare that they have no known competing financial interests or personal relationships that could have appeared to influence the work reported in this paper.

Acknowledgements

The present research was supported by the PhD Fellowship DOT1316197 (IMTR) CUP D45F21003710001 (Green) financed by Italian PON “Ricerca e Innovazione” 2014–2020 funding program. The authors also acknowledge funding from the European Union’s Horizon 2020 research and innovation programme under Marie Skłodowska-Curie project SUBLime [Grant Agreement n°955986]; the Spanish

Government grant PID2021.125305NB.I00 funded by MCIN/ AEI /10.13039/501100011033 and by ERDF A way of making Europe; Junta de Andalucía research group RNM-179; and University of Granada, Unidad Científica de Excelencia UCE-PP2016–05. The authors would like to thank Samuele Beraldo, Andrea Bettiol and Marco Bobba from Fassa I-Lab Ricerca & Sviluppo Fassa Srl, for the availability and help in the experimental analysis of the quicklime characterization with XRD. The authors also thank Irene De Giuli and Maria Sugari for their support in the experimental activities. Finally, the authors would like to thank Fassa Bortolo Srl and Weidmann Fiber Technology for providing some of the materials used in this work.

Appendix A. Supporting information

Supplementary data associated with this article can be found in the online version at doi:10.1016/j.conbuildmat.2025.142291.

Data Availability

Data will be made available on request.

References

- [1] A. Laveglia, N. Ukrainczyk, N. De Belie, E. Koenders, From quarry to carbon sink: process-based LCA modelling of lime-based construction materials for net-zero and carbon-negative transformation, *Green. Chem.* (2024).
- [2] A. Laveglia, D.V. Madrid, N. Ukrainczyk, V. Cnudde, N. De Belie, E. Koenders, Circular design, material properties, service life and cradle-to-cradle carbon footprint of lime-based building materials, *Sci. Total Environ.* 948 (2024) 174875.
- [3] A. Isebaert, L. Van Parys, V. Cnudde, Composition and compatibility requirements of mineral repair mortars for stone – a review, *Constr. Build. Mater.* 59 (2014) 39–50, <https://doi.org/10.1016/J.CONBUILDMAT.2014.02.020>.
- [4] R. Veiga, Air lime mortars: what else do we need to know to apply them in conservation and rehabilitation interventions? A review, *Constr. Build. Mater.* 157 (2017) 132–140, <https://doi.org/10.1016/J.CONBUILDMAT.2017.09.080>.
- [5] C. Groot, R. Veiga, I. Papayianni, R. Van Hees, M. Secco, J.I. Alvarez, P. Faria, M. Stefanidou, R.L.L.E.M. TC, 277-LHS report: lime-based mortars for restoration—a review on long-term durability aspects and experience from practice, *Mater. Struct.* 55 (2022) 245.
- [6] A. Henry, J. Stewart, E. Heritage, *Practical building conservation: mortars, renders and plasters*, 2011.
- [7] R.S. Boynton, *Chemistry and technology of lime and limestone*, 1966.
- [8] K. Van Balen, D. Van Gemert, Modelling lime mortar carbonation, *Mater. Struct.* 27 (1994) 393–398, <https://doi.org/10.1007/BF02473442>.
- [9] C. Rodríguez-Navarro, T. Ilić, E. Ruiz-Agudo, K. Elert, Carbonation mechanisms and kinetics of lime-based binders: an overview, *Cem. Concr. Res.* 173 (2023) 107301.
- [10] Ö. Cizer, K. Van Balen, J. Elsen, D. Van Gemert, Real-time investigation of reaction rate and mineral phase modifications of lime carbonation, *Constr. Build. Mater.* 35 (2012) 741–751.
- [11] Ö. Cizer, E. Ruiz-Agudo, C. Rodríguez-Navarro, Kinetic effect of carbonic anhydrase enzyme on the carbonation reaction of lime mortar 12 (2018) 779–789, <https://doi.org/10.1080/15583058.2017.1413604>.
- [12] O. Cazalla, C. Rodríguez-Navarro, E. Sebastian, G. Cultrone, M.J. De la Torre, Aging of lime putty: effects on traditional lime mortar carbonation, *J. Am. Ceram. Soc.* 83 (2000) 1070–1076.
- [13] D. Wang, J. Xiao, Z. Duan, Strategies to accelerate CO₂ sequestration of cement-based materials and their application prospects, *Constr. Build. Mater.* 314 (2022) 125646.
- [14] C. Rodríguez-Navarro, E. Ruiz-Agudo, M. Ortega-Huertas, E. Hansen, Nanostructure and irreversible colloidal behavior of Ca (OH) 2: implications in cultural heritage conservation, *Langmuir* 21 (2005) 10948–10957.
- [15] D. Ergenç, R. Fort, Accelerating carbonation in lime-based mortar in high CO₂ environments, *Constr. Build. Mater.* 188 (2018) 314–325.
- [16] P.N. Maravelaki, K. Kapetanaki, I. Papayianni, I. Ioannou, P. Faria, J. Alvarez, M. Stefanidou, C. Nunes, M. Theodoridou, L. Ferrara, R.L.L.E.M. TC, 277-LHS report: additives and admixtures for modern lime-based mortars, *Mater. Struct.* 56 (2023) 106.
- [17] I. Karatasios, M.S. Katsiotis, V. Likodimos, A.I. Kontos, G. Papavassiliou, P. Falaras, V. Kilikoglou, Photo-induced carbonation of lime-TiO₂ mortars, *Appl. Catal. B* 95 (2010) 78–86, <https://doi.org/10.1016/J.APCATB.2009.12.011>.
- [18] P. Maravelaki-Kalaitzaki, Z. Agioutantis, E. Lionakis, M. Stavroulaki, V. Perdikatsis, Physico-chemical and mechanical characterization of hydraulic mortars containing nano-titanium for restoration applications, *Cem. Concr. Compos* 36 (2013) 33–41, <https://doi.org/10.1016/J.CEMCONCOMP.2012.07.002>.
- [19] K. Kapetanaki, C. Kapridaki, P.-N. Maravelaki, Nano-TiO₂ in hydraulic lime–metakaolin mortars for restoration projects: physicochemical and mechanical assessment, *Buildings* 9 (2019) 236.

- [20] S. Jayasingh, T. Selvaraj, S. Raneri, Evaluating the impact of organic addition and aggregate gradation on air lime mortar, *N. Compat. Green. Mater. Herit. Appl.* (2020), <https://doi.org/10.1080/15583058.2020.1836287>.
- [21] S. Jayasingh, T. Selvaraj, Influence of organic additive on carbonation of air lime mortar – changes in mechanical and mineralogical characteristics, *Eur. J. Environ. Civil. Eng.* (2020), <https://doi.org/10.1080/19648189.2020.1731716>. <https://doi.org/10.1080/19648189.2020.1731716>.
- [22] A. Manoharan, C. Umarani, Properties of air lime mortar with bio-additives, *Sustainability* 14 (2022) 8355.
- [23] D. Ergenç, R. Fort, A. Santos Silva, R. Veiga, D. Sanz Arauz, The effects of DiloCarB as carbonation accelerator on the properties of lime mortars, *Mater. Struct. /Mater. Et. Constr.* 51 (2018) 1–16, <https://doi.org/10.1617/S11527-018-1140-0/FIGURES/8>.
- [24] C. Rodríguez-Navarro, L. Monasterio-Guillot, M. Burgos-Ruiz, E. Ruiz-Agudo, K. Elert, Unveiling the secret of ancient Maya masons: biomimetic lime plasters with plant extracts, *Sci. Adv.* 9 (2023) eadf6138.
- [25] C. Rodríguez-Navarro, E. Ruiz-Agudo, A. Burgos-Cara, K. Elert, E.F. Hansen, Crystallization and colloidal stabilization of Ca(OH)₂ in the presence of nopal juice (*Opuntia ficus indica*): implications in architectural heritage conservation, *Langmuir* 33 (2017) 10936–10950, https://doi.org/10.1021/ACS.LANGMUIR.7B02423/SUPPL_FILE/LA7B02423_SI_001.PDF.
- [26] C. Rodríguez-Navarro, A. Burgos-Cara, F. Di Lorenzo, E. Ruiz-Agudo, K. Elert, Nonclassical crystallization of calcium hydroxide via amorphous precursors and the role of additives, *Cryst. Growth Des.* 20 (2020) 4418–4432, https://doi.org/10.1021/ACS.CGD.0C00241/ASSET/IMAGES/LARGE/CGOC00241_0007.JPEG.
- [27] M.G. Margalha, A.S. Silva, M. do Rosário Veiga, J. De Brito, R.J. Ball, G.C. Allen, Microstructural changes of lime putty during aging, *J. Mater. Civ. Eng.* 25 (2013) 1524–1532.
- [28] A. Formisano, G. Chiumiento, E.J. Dessì, Laboratory tests on hydraulic lime mortar reinforced with jute fibres, *Open Civ. Eng. J.* 14 (2020) 152–162, <https://doi.org/10.2174/1874149502014010152>.
- [29] F. Kesikidou, M. Stefanidou, Natural fiber-reinforced mortars, *J. Build. Eng.* 25 (2019) 100786, <https://doi.org/10.1016/J.JOBE.2019.100786>.
- [30] M. Stefanidou, V. Kamperidou, A. Konstantinidis, P. Koltso, S. Papadopoulos, Use of *Posidonia oceanica* fibres in lime mortars, *Constr. Build. Mater.* 298 (2021) 123881, <https://doi.org/10.1016/J.CONBUILDMAT.2021.123881>.
- [31] M. Vailati, M. Mercuri, M. Angiolilli, A. Gregori, Natural-fibrous lime-based mortar for the rapid retrofitting of heritage masonry buildings, *Fibers* 2021 9 (2021) 68, <https://doi.org/10.3390/FIB9110068>.
- [32] E. Vismara, G. Bertolini, C. Bongio, N. Massironi, M. Zarattini, D. Nanni, C. Cosentino, G. Torri, Nanocellulose from cotton waste and its glycidyl methacrylate grafting and allylation: synthesis, characterization and adsorption properties, *Nanomaterials* 2021 11 (2021) 476, <https://doi.org/10.3390/NANO11020476>.
- [33] L. Rosato, M. Stefanidou, G. Milazzo, F. Fernandez, P. Livreri, N. Muratore, L. M. Terranova, Study and evaluation of nano-structured cellulose fibers as additive for restoration of historical mortars and plasters, *Mater. Today Proc.* 4 (2017) 6954–6965, <https://doi.org/10.1016/J.MATPR.2017.07.025>.
- [34] C. D'Erme, W.R. Caseri, M.L. Santarelli, Effect of fibrillated cellulose on lime pastes and mortars, 459, *Materials* 2022 15 (2022) 459, <https://doi.org/10.3390/MA15020459>.
- [35] P. Guzmán García Lascurain, C. Rodríguez-Navarro, L. Toniolo, S. Goidanich, Effects of nano-and micro-cellulose on Ca (OH)₂ formation: implications for lime-based binders, *Cem. Concr. Res* 192 (2025) 107851.
- [36] P.G.G. Lascurain, C. Rodríguez-Navarro, I. De Giuli, L. Toniolo, S. Goidanich, Study of the influence of micro-and nano-cellulose on the growth and carbonation kinetics of portlandite crystals, *MATEC Web Conf. EDP Sci.* (2024) 03009.
- [37] R. Ciriminna, G. Angellotti, G.L. Petri, F. Meneguzzo, C. Riccucci, G.Di Carlo, M. Pagliaro, Cavitation as a zero-waste circular economy process to convert citrus processing waste into biopolymers in high demand, *J. Bioresour. Bioprod.* 9 (2024) 486–494.
- [38] A. Scurria, L. Albanese, M. Pagliaro, F. Zabini, F. Giordano, F. Meneguzzo, R. Ciriminna, CytroCell: valued cellulose from citrus processing waste, *Molecules* 2021 26 (2021) 596, <https://doi.org/10.3390/MOLECULES26030596>.
- [39] H.M. Rietveld, A profile refinement method for nuclear and magnetic structures, *Appl. Crystallogr.* 2 (1969) 65–71.
- [40] E. Despotou, A. Shtiza, T. Schlegel, F. Verhelst, Literature study on the rate and mechanism of carbonation of lime in mortars/Literaturstudie über Mechanismus und Grad der Karbonatisierung von Kalkhydrat im Mörtel, *Mauerwerk* 20 (2016) 124–137.
- [41] J.J. Thomas, A new approach to modeling the nucleation and growth kinetics of tricalcium silicate hydration, *J. Am. Ceram. Soc.* 90 (2007) 3282–3288.
- [42] J.W. Cahn, The kinetics of grain boundary nucleated reactions, *Acta Metall.* 4 (1956) 449–459.
- [43] R. Camerini, G. Poggi, D. Chelazzi, F. Ridi, R. Giorgi, P. Baglioni, The carbonation kinetics of calcium hydroxide nanoparticles: a boundary nucleation and growth description, *J. Colloid Interface Sci.* 547 (2019) 370–381.
- [44] F.A. Andersen, L. Brecevic, G. Beuter, D.B. Dell'Amico, F. Calderazzo, N.J. Bjerrum, A.E. Underhill, Infrared spectra of amorphous and crystalline calcium carbonate, *Acta Chem. Scand.* 45 (1991) 1018–1024.
- [45] D. Gebauer, M. Kellermeier, J.D. Gale, L. Bergström, H. Cölfen, Pre-nucleation clusters as solute precursors in crystallisation, *Chem. Soc. Rev.* 43 (2014) 2348–2371.
- [46] H. Fu, X. Gao, X. Zhang, L. Ling, Recent advances in nonclassical crystallization: fundamentals, applications, and challenges, *Cryst. Growth Des.* 22 (2021) 1476–1499.
- [47] A. Scurria, M. Pagliaro, G. Pantaleo, F. Meneguzzo, F.M. Giordano, R. Ciriminna, CytroCell micronized cellulose enhances the structural and thermal properties of IntegroPectin cross-linked films, *ACS Appl. Bio Mater.* 5 (2022) 4942–4947.
- [48] A.A.B. Omran, A.A.B.A. Mohammed, S.M. Sapuan, R.A. Ilyas, M.R.M. Asyraf, S. S. Rahimian Kolor, M. Petri, Micro-and nanocellulose in polymer composite materials: a review, *Polymers* 13 (2021) 231.
- [49] A.-S.F. Tixier, N. Michel, R. Ciriminna, G.L. Petri, G. Angellotti, A.R. Garcia, M. Pagliaro, CytroCell in aqueous solution: a computational and DRIFT spectroscopy, *Insight* (2025).
- [50] R.K. Walzel, V.I. Levitas, M.L. Pantoya, Aluminum particle reactivity as a function of alumina shell structure: amorphous versus crystalline, *Powder Technol.* 374 (2020) 33–39.
- [51] C. Bhugra, M.J. Pikal, Role of thermodynamic, molecular, and kinetic factors in crystallization from the amorphous state, *J. Pharm. Sci.* 97 (2008) 1329–1349.
- [52] R.A. Bellantone, Fundamentals of amorphous systems: thermodynamic aspects, *Amorph. Solid Dispers. Theory Pract.* (2014) 3–34.
- [53] L.D. Landau, E.M. Lifshitz, *Statistical Physics: Volume 5*, Elsevier, 2013.
- [54] C. Rodríguez-Navarro, E. Hansen, W.S. Ginell, Calcium hydroxide crystal evolution upon aging of lime putty, *J. Am. Ceram. Soc.* 81 (1998) 3032–3034.
- [55] C. Pesce, R.J. Ball, M. Molinari, S. Reeksting, G.L. Pesce, Effects of carbohydrates and sulfonates during CaO hydration on portlandite microstructure, *Cem. Concr. Res.* 175 (2024) 107372.
- [56] Z. Deng, Z. Jia, L. Li, Biomineralized materials as model systems for structural composites: intracrystalline structural features and their strengthening and toughening mechanisms, *Adv. Sci.* 9 (2022) 2103524.
- [57] Z. Deng, L. Chen, L. Li, Comparative nanoindentation study of biogenic and geological calcite, *J. Mech. Behav. Biomed. Mater.* 137 (2023) 105538.
- [58] Q. Lu, Z. Cai, S. Wang, F. Lin, B. Lu, Y. Chen, B. Huang, Controlled construction of nanostructured organic–inorganic hybrid material induced by nanocellulose, *ACS Sustain Chem. Eng.* 5 (2017) 8456–8463, <https://doi.org/10.1021/ACSUSCHEMENG.7B02394>.